PHYSICAL REVIEW B VOLUME 49, NUMBER 15 15 APRIL 1994-I

Shubnikov–de Haas oscillations under hot-electron conditions in $Si/Si_{1-x}Ge_x$ heterostructures

G. Stöger, G. Brunthaler, and G. Bauer
Institut für Halbleiterphysik, Universität Linz, A-4040 Linz, Austria

K. Ismail* and B. S. Meyerson
IBM Thomas J. Watson Research Center, Yorktown Heights, New York 10598

J. Lutz and F. Kuchar
Institut für Physik, Montanuniversität Leoben, A-8700 Loeben, Austria
(Received 27 May 1993; revised manuscript received 17 November 1993)

The energy-loss rate of hot carriers in several modulation-doped $Si/Si_{1-x}Ge_x$ heterostructures has been studied. The Ohmic properties of the $Si/Si_{1-x}Ge_x$ samples, which were grown by ultrahigh-vacuum chemical-vapor deposition, were studied by Hall effect, conductivity, Shubnikov–de Haas, and quantum Hall effect measurements. For the samples with mobilities ranging from 1.3×10^4 to 1.3×10^5 cm^2/Vs at $T\approx2$ K the ratio of the transport time to the single-particle scattering time increases from 2.4 to 7.7. This result clearly indicates the change from dominant short-range to rather long-range scattering mechanisms in the higher quality $Si/Si_{1-x}Ge_x$ heterostructures. The dependence of the energy-loss rate (P_E) on electron temperature (T_e) was obtained from the damping of the Shubnikov–de Haas oscillations with applied electric field up to 5 V/cm. In the electron temperature range from 1.6 to 7 K, the functional dependence of P_E does not change when the mobility of the samples is varied by a factor of 10, and thus $P_E(T_e)$ is unaffected by the nature of the elastic-scattering mechanisms within these limits. In this electron temperature range the dominant energy-loss mechanism is due to acoustic-phonon scattering via deformation-potential coupling. For a deformation-potential coupling constant of 9 eV, taking static screening into account, a quantitative agreement between experimental and calculated values of the energy-loss rate is obtained without any fit parameter.

I. INTRODUCTION

Recent advances in epitaxial growth techniques of $Si/Si_{1-x}Ge_x$ heterostructures have resulted in high-mobility two-dimensional electron (2DEG) and hole gases.[1–4] These heterostructures are of considerable importance for possible device applications. Heterobipolar (HBT) as well as two-dimensional electron-gas field-effect transistors (TEGFET's) were realized by groups at IBM (Refs. 5–7) and Daimler Benz.[8,9] Since the carrier mobilities in modulation-doped $Si/Si_{1-x}Ge_x$ samples available exceed those of Si–metal-oxide semiconductor (MOS) devices by far, studies of carrier transport which were previously restricted mainly to the $GaAs/Ga_{1-x}Al_xAs$ system can be performed nowadays too.

It is the purpose of this paper to report hot-carrier studies in several modulation-doped n-type $Si/Si_{1-x}Ge_x$ heterostructures at low temperature. In order to achieve a two-dimensional electron channel, the conduction-band edge of Si has to be lowered with respect to that of $Si_{1-x}Ge_x$.[10,11] The typical way of achieving this requirement is by growing a relaxed $Si_{1-x}Ge_x$ alloy or superlattice buffer[2] on which the Si layer is under biaxial tensile strain. The Ge concentration in the buffer, the sequence of layers in the buffer, and its total thickness determine the density of threading dislocations, which result from the relaxation process due to the Si-Ge lattice constant mismatch ($\Delta a/a\approx4\%$), and diminish the electron mobility.

We have measured the energy-loss rate in samples where both the buffer thickness and the thickness of the nominally undoped $Si_{1-x}Ge_x$ spacer layer were changed in order to achieve a transition from comparatively low (1.3×10^4 $cm^2/V\,s$) to high-mobility (1.3×10^5 $cm^2/V\,s$) behavior. Theoretically the low-temperature electron mobilities and densities in modulation-doped $Si/Si_{0.7}Ge_{0.3}$ heterostructures were studied by Stern and Laux[12] as a function of spacer thickness. Gold[13] has pointed out that, due to the high value of the longitudinal mass ($m_z\equiv m_l=0.92m_0$), in high-quality $Si/Si_{1-x}Ge_x$ structures, interface scattering should not be of considerable importance in Si quantum wells (QW's) wider than 60 Å. High-quality $Si/Si_{1-x}Ge_x$ heterostructures have mobilities which are superior to even the best Si MOSFET's reported so far. $Si/Si_{1-x}Ge_x$ heterostructures possess the potential to replace Si MOS structures for certain applications in the future. In such devices, due to their small characteristic lengths, the applied voltage inevitably causes hot-electron phenomena to occur. Consequently it is desirable to understand the non-Ohmic transport in $Si/Si_{1-x}Ge_x$ heterostructures.

In this paper we report a study of the energy-loss rate in three modulation-doped $Si/Si_{1-x}Ge_x$ samples. The experimental results are compared with calculations of the energy-loss rate due to acoustic-phonon scattering including static screening effects. In addition, the present results obtained for the $Si/Si_{1-x}Ge_x$ heterostructures are compared to previous experimental and theoretical data

0163-1829/94/49(15)/10417(9)/$06.00 ©1994 The American Physical Society

for Si MOS structures.

In order to determine the relevant energy-loss mechanisms of hot carriers at low lattice temperatures, the determination of their electron temperature as a function of applied electric field is a commonly used technique. At liquid-helium temperatures this dependence can be obtained from the measurement of the damping of the amplitudes of Shubnikov–de Haas oscillations in relatively small magnetic fields.

This technique was originally used for three-dimensional[14] electron systems, and was later adopted for studies of two-dimensional electron systems in $GaAs/Ga_{1-x}Al_xAs$ (Refs. 15–19) and Si MOSFET's.[20,21] Furthermore, in high-mobility $GaAs/Ga_{1-x}Al_xAs$ heterostructures a quantum correction to the conductivity, which is due to electron-electron interaction, was observed in the magnetic-field range of the nonoscillatory magnetoresistance.[22] The suppression of the electron-electron interaction in the hot-electron regime has been used to determine the electron temperature T_e as well.

II. EXPERIMENTAL DETAILS

The three $Si/Si_{1-x}Ge_x$ heterostructures investigated in this study were grown at 550 °C on high-resistivity p^- substrates using an ultrahigh-vacuum chemical-vapor deposition (UHV-CVD) system. Figure 1 shows a sketch of the sample cross section together with the conduction-band diagram. A 500-nm-thick, $Si/Si_{1-x}Ge_x$ superlattice (SL) buffer with an average Ge content of 0.3 is grown to serve as a strain relief multilayer.[2] Above the SL either a partly relaxed 50-nm or fully relaxed 1500-nm-thick $Si_{0.7}Ge_{0.3}$ alloy buffer is grown which determines the strain status of the subsequent layers. Then follows the 10-nm-wide tensily strained Si layer, and an either 4- or 15-nm-wide $Si_{0.7}Ge_{0.3}$ spacer layer. The phosphorus-doped supply layer ($Si_{0.8}Ge_{0.2}$,$N_D=4\times10^{18}$ cm^{-3}) is followed by a sequence of three cap layers: a $Si_{0.7}Ge_{0.3}$ layer, a second 4-nm-thick ($N_D=2\times10^{18}$ cm^{-3}) supply layer, and on top a 2-nm-thick Si layer. The second supply layer is used to prevent depletion by the surface potential.[2,23]

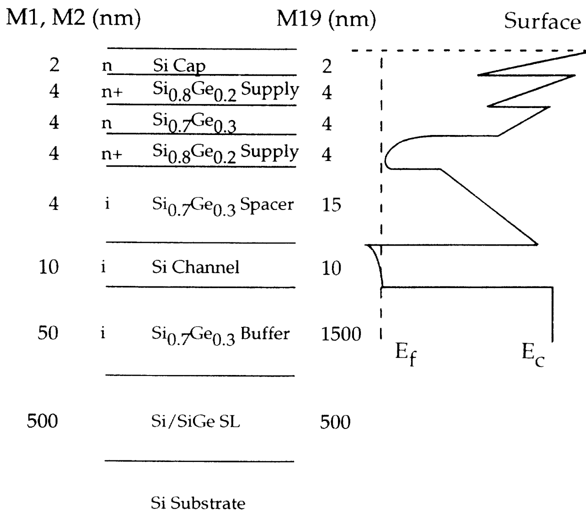

FIG. 1. Sketch of the sample structure, with layer thicknesses given in nm for samples $M1$, $M2$, and $M19$ as well as the conduction-band diagram.

Since the Si channel experiences tensile strain in the structures, the sixfold-degenerate levels are split into doubly degenerate Δ_2 and fourfold-degenerate Δ_4 states. The lowest-lying states are the Δ_2 states, which are oriented with their main axis perpendicular to the (001) surface. The longitudinal mass is given by $m_z=0.92m_0$, and the transversal in-plane mass by $m_t=0.19m_0$. For this situation the two-dimensional electron gas is confined in a triangular-shaped potential well.[12] For the three samples investigated (which are labeled $M1$, $M2$, and $M19$) all electrons are in the lowest subband, as deduced from Fourier analysis of the Shubnikov–de Haas oscillations. The carriers are located on the side of the Si layer which is closer to the supply layer. The conduction-band offset is known to be about 120–150 meV; the exact value depends on the amount of strain relaxation in the buffer layers. The main differences between samples $M1$ and $M2$ on the one hand, and $M19$ on the other, are the thicknesses of the buffer and spacer layers, which have been increased from 50 to 1500 nm and from 4 to 15 nm, respectively (Fig. 1). This reduces the amount of carrier transfer into the 2DEG channel from 9.8×10^{11} cm^{-2} ($M1$) to about 4.7×10^{11} cm^{-2} ($M19$) and increases the low-temperature mobility from about 1.3×10^4 ($M2$) to 1.3×10^5 $cm^2/V\,s$ ($M19$). The sample parameters are listed in Table I.

As pointed out by Nelson *et al.*[23] and Xie *et al.*[4], the low-temperature mobility in the 2D channels grown on thick buffers is not limited by the density of threading dislocations for densities less than 10^8 cm^{-2}. In high-mobility UHV-CVD samples comparable to $M19$, the threading-dislocation density was determined to be on the order of 10^7 cm^{-2} (Ref. 23).

The transport measurements were performed on lithographically defined Hall bars with a channel width of either 140 ($M1$,$M2$) or 75 μm ($M19$) and a channel length of 450 ($M1$,$M2$) or 1500 μm ($M19$). The voltage drop was measured with voltage probes 200 or 750 μm apart. Ohmic contacts of an AuSb alloy were used for all samples. For samples $M1$ and $M19$ the contacts were annealed at 300 °C, whereas for sample $M2$ they were not.

TABLE I. Carrier concentration, Hall mobility, Fermi energy, Dingle temperature, and scattering times after illumination at $T\approx2$ K for low electric fields.

Sample	$M1$	$M2$	$M19$
n (10^{12} cm^{-2})	0.98	0.88	0.47
μ ($cm^2/V\,s$)	1.43×10^4	1.31×10^4	1.32×10^5
E_F (meV)	6.2	5.6	3.0
T_D (K)	1.9	2.5	0.67
τ_s (ps)	0.64	0.49	1.8
τ_t (ps)	1.55	1.42	14.3
τ_t/τ_s	2.4	2.9	7.9

Later it was found that samples $M1$ and $M19$ were sensitive to band-gap illumination at low temperatures and showed persistent conductivity effects, whereas sample $M2$ did not exhibit any detectable sensitivity to illumination.

Hall-effect investigations were performed in a bath cryostat at 4.2 K, and in a continuous-flow cryostat with variable-temperature control at magnetic fields of typically 0.35 T.

Shubnikov–de Haas (SdH) oscillations were recorded under constant-current conditions for a magnetic field applied perpendicular to the plane of the 2DEG. Increasing lattice or electron temperature damps the Shubnikov–de Haas oscillations through thermal broadening, i.e., through changing the ratio $\hbar\omega_c/k_BT_e$ ($\hbar\omega_c$ is the cyclotron energy), which crucially determines the oscillatory magnetoresistance.[24] Hence the SdH amplitudes depend explicitly on the electron temperature T_e but not on the lattice temperature T_L. The electron temperatures at higher input power are determined by comparing the ratio of the resulting amplitudes to the amplitude obtained under Ohmic conditions (at $T_e \approx 2$ K) with theory according to the procedure outlined by Bauer and Kahlert.[14] It is assumed that the Dingle temperature T_D remains constant and does not change with electric field. Under Ohmic conditions, we found no dependence of the Dingle temperature on lattice temperature in the range from $T_L = 1.6$–4.2 K.

For comparison, the damping of the SdH oscillations was measured at a higher lattice temperature of 4.2 K and low input power (i.e., in the Ohmic regime). These calibration data at 4.2 K are in good agreement with the electron temperatures evaluated from the damping of the SdH oscillations at higher input power. Indeed, this calibration procedure relies on the fact that the amplitudes of the SdH oscillations depend on the electron temperature which appears in the electron distribution function.

Due to the resistivity oscillations, the electric field between the voltage probes is not constant, but for small SdH oscillations the deviations are only in the percent range. The SdH measurements under hot-electron conditions were performed at a lattice temperature of about 2 K. The currents were of the order of 0.1–100 μA, corresponding to electric fields in the range from 1 mV/cm to 5 V/cm. For lower electric fields no change in the damping of the SdH oscillations was observed.

For the evaluation of the data it has to be considered that the calculation of the energy-loss rate used below is based on the assumption of a constant 2D density of states. The SdH oscillations occur in a regime where the magnetic field alters the 2D density of states and hence also the scattering rates of the carriers. In order to keep this disturbance small, the magnetic field for the evaluation of the SdH oscillations has to be restricted to sufficiently small values so that $\Delta R^{\mathrm{SdH}}/R$ is of the order of a few percent.

III. OHMIC TRANSPORT

The samples were characterized by Hall-effect and conductivity measurements. The resulting temperature dependences of carrier concentration and Hall mobility for the low-mobility sample $M1$ and high-mobility sample $M19$ are shown in Fig. 2. The room-temperature mobilities were about 1200 and 2000 cm^2/V s, respectively. At low temperatures, both samples displayed in Fig. 2 show a persistent increase of electron mobility after illumination with a GaAs light-emitting diode (LED) ($\lambda = 950$ nm). There is a difference between the heating and cooling curves for temperatures up to about 100 K. For higher temperatures the persistent or metastable effects present in mobility as well as in carrier concentration vanish. The Hall data for sample $M2$ are comparable to those of sample $M1$, but they do not show any sensitivity to band-gap illumination. Due to the sensitivity

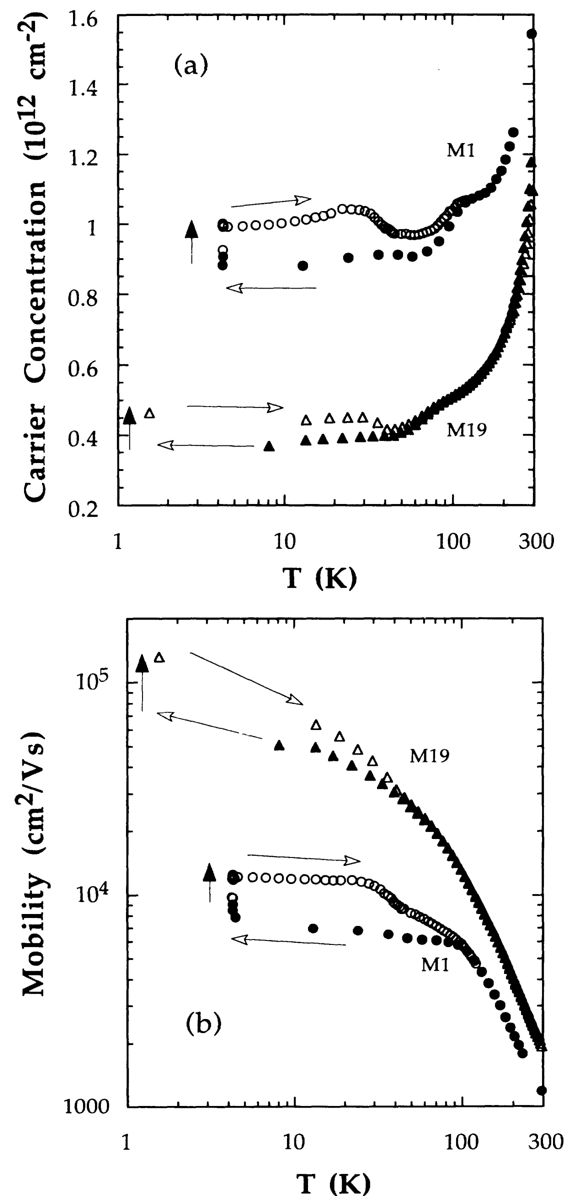

FIG. 2. Carrier concentration (a) and Hall mobility (b) vs temperature of samples $M1$ and $M19$ during cooling from room temperature to 4 or 1.8 K before illumination (full symbols), and during warming up after illumination (open symbols).

of samples $M1$ and $M19$ to band-gap radiation, all transport measurements were recorded after illumination at low temperatures.

As an explanation for the sensitivity of these samples to illumination with band-gap radiation, we suggest a process where ionized impurities, located close to the 2D electrons, are neutralized. During illumination, free carriers are excited into high-energy states above the band offset between SiGe and Si layers. From there some carriers will enter the SiGe barrier layer and will be able to neutralize local defects. A similar charge transfer across heterojunctions was observed in $Al_xGa_{1-x}As/GaAs$ quantum wells during illumination.[25]

In order to characterize the samples further, the resistivity and Hall effect of the low-mobility samples $M1$ and $M2$ were measured at $T=1.8$ K up to magnetic fields of 16 T. These results are shown for sample $M2$ at $T=1.8$ K in Fig. 3. For filling factors between $\nu=4$ and 8 the spin splitting is clearly resolved in ρ_{xx}. For higher magnetic fields ρ_{xx} shows the results of the lifting of the twofold valley degeneracy at the odd filling factor $\nu=3$. For magnetic fields $B<4$ T, the magnetoresistance oscillations correspond to filling factors which are multiples of 4 (since neither the twofold spin splitting nor the twofold valley splitting is resolved). From the values of the $\nu=4$ and 8 integer quantum Hall plateaus, one concludes that the amount of parallel conduction is negligible. The carrier concentrations evaluated from the SdH oscillations are, within experimental error, identical to those obtained from the Hall measurements on all samples, which further proves that parallel conduction is negligible at low temperatures.

The Dingle temperature T_D is deduced from the damping of the SdH oscillations as a function of magnetic field. For the low-mobility samples $M1$ and $M2$ we obtained $T_D=1.9$ and 2.5 K, and for the high-mobility sample $M19$ a value of $T_D=0.67$ K (Table I).

The ratio of transport relaxation time τ_t to the single-particle relaxation time τ_s (or quantum lifetime τ_q) deduced from the Dingle temperature T_D yields information about the dominant scattering mechanism.[12,26–28] The time τ_s describes a Lorentzian broadening of the Landau levels due to scattering of electrons. The two characteristic times are calculated from $\mu=e\tau_t/m_t$ and $\hbar/2\pi\tau_s=k_BT_D$, respectively, where e is the elementary charge, $m_t=0.19m_0$ is the effective transverse mass of conduction-band electrons, and $\hbar$ is Planck's constant. The single-particle or quantum lifetime is determined by the total scattering rate

$$\frac{1}{\tau_s}=\int W(\mathbf{k},\mathbf{k}')d\theta \;, \qquad (1)$$

where $W(\mathbf{k},\mathbf{k}')$ is the transition rate for scattering from wave vector $\mathbf{k}$ into $\mathbf{k}'$ and θ denotes the scattering angle. In the relaxation time ansatz for solving the Boltzmann transport equation, the transport relaxation time is given by

$$\frac{1}{\tau_t}=\int W(\mathbf{k},\mathbf{k}')(1-\cos\theta)d\theta \;, \qquad (2)$$

i.e., it is weighted by the scattering angle. Coleridge, Stoner, and Fletcher[27] and Das Sarma and Stern[26] have pointed out that for a short-range scattering potential the ratio τ_t/τ_s is close to unity, whereas for long-range scattering this ratio is much larger. Indeed, for remote impurity scattering in modulation-doped $GaAs/Ga_{1-x}Al_xAs$ structures, this ratio was found to be 10 or more.

For sample $M1$ we determined a ratio $\tau_t/\tau_s=2.4$, while for sample $M2$ we obtained a value of $\tau_t/\tau_s=2.9$. From these ratios we conclude that in samples $M1$ and $M2$, where the spacer thickness is 4 nm, remote impurity scattering definitely does not limit the mobility. According to Stern and Laux[12] a ratio τ_t/τ_s of about 6–7 is expected for these particular samples. Consequently other scattering mechanisms limit the mobility, such as unintentional impurities in the 2DEG channel or the spacer layer, or scattering due to interface roughness.

For the high-mobility sample $M19$ the ratio τ_t/τ_s is about 8. For a spacer layer of 15 nm, τ_t/τ_s values well above 10 would be expected from the calculations in Ref. 12. Based on these calculations one cannot draw the conclusion that the mobility in the high-mobility sample is limited by remote impurity scattering only. The influence of interface roughness on the mobility is not yet well established.[12] Gold has calculated values of the electron mobility limited by interface roughness in $Si/Si_{1-x}Ge_x$ rectangular quantum wells for several well widths ranging from 40 to 120 Å.[13] He obtained limiting values for μ of about 10^4 cm^2/V s for the 40-Å wells, and about 10^5 cm^2/V s for the 60-Å wells. However, these results are not applicable for a direct comparison with the data on one-sided modulation-doped $Si/Si_{1-x}Ge_x$ structures. Gold's result was obtained assuming a symmetric, sinusoidal wave function of the ground state which vanishes at the boundaries. In a triangular potential well, the probability of finding the electron in the lowest subband close to the interface is higher compared to that of a square well with infinitely high potential boundaries.

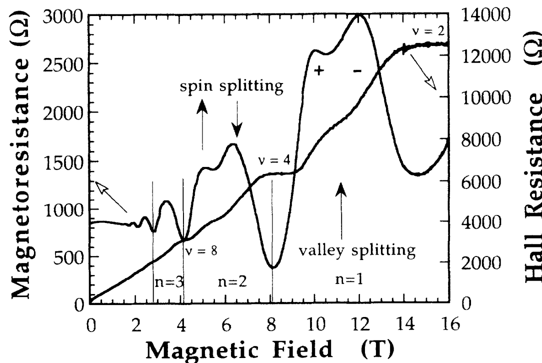

FIG. 3. SdH oscillations and quantum Hall effect for sample $M2$ at $T=1.8$ K. Spin split states ($\uparrow/\downarrow$) of the second Landau level $n=2$ and valley splitting ($+/-$) for $n=1$ are clearly observable. Hall plateaus are indicated for filling factors $\nu=2$, 4, and 8.

IV. NON-OHMIC TRANSPORT

The damping of the amplitudes of the Shubnikov–de Haas oscillations with increasing electric field was used to determine the electron temperature. For these measurements the lattice temperature was kept constant, i.e., the samples were kept immersed in superfluid helium at a bath temperature of $T=1.8$ K for sample $M1$, $T=2.1$ K for sample $M2$, and $T=1.55$ K for sample $M19$.

The electric fields employed are so small (less than 2 V/cm, 5 V/cm, and 300 mV/cm for the three samples $M1$, $M2$, and $M19$, respectively) that there is no appreciable population of the second electric subband at all, i.e., a Fourier analysis of the SdH data reveals that even at the maximum electric fields only the lowest electron subband is occupied. At much higher fields ($F>8$ V/cm) an increase in the mobility was observed, which is attributed to a population of the second subband, similar to results of investigations on Si MOS structures.[29]

The data of the experimentally obtained energy-loss rate as a function of T_e for the three samples are shown in Fig. 4, and are denoted by the open symbols. In steady state, the loss rate per electron P_E equals the input power which is given by $P_E=U^2/RN_e=e\mu F^2$, where R is the sample resistance, U the voltage drop, and N_e the total number of electrons. The mobility μ varies with applied electric field F by roughly 15% (measured at zero magnetic field at $T_L=2$ K) and has to be considered for the evaluation.

It is worth pointing out that $P_e(T_e)$ is nearly identical for all three samples, despite the factor of 10 difference in electron mobility and thus also in the power input for a given electric field. These data prove that the energy-loss rate is virtually unaffected by the elastic scattering mechanisms, as should be the case in a model where the hot-carrier distribution function is a Fermi distribution function with T_e replacing T_L. To the best of our knowledge, the dependence of P_E (T_e) has not been investigated for such a wide range of 2DEG mobilities in $GaAs/Ga_{1-x}Al_xAs$ or Si MOS devices.

In Fig. 4 experimental data on P_E (T_e) obtained by the same method on Si MOS structures by Neugebauer and Landwehr[20] are shown as well. Their sample P77M2PP had a sheet electron density of $n=3.7\times10^{12}$ cm^{-2} and an electron mobility of $\mu=4000$ cm^2/V s (Ref. 30) at $T_L=1.7$ K. There is an apparent difference between experimental results for $Si/Si_{1-x}Ge_x$ heterostructures and the Si MOS devices which will be discussed in Sec. VI.

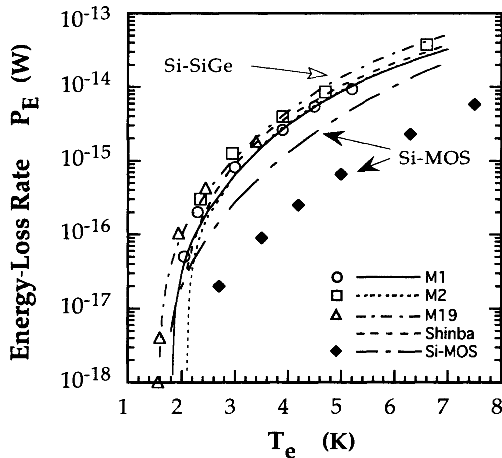

FIG. 4. Energy-loss rate P_E vs electron temperature T_e determined for a lattice temperature of $T_L=1.8$ K for sample $M1$ (circles), 2.1 K for sample $M2$ (squares), and 1.55 K for sample $M19$ (triangles). The data for a Si MOS device from Ref. 20 (full diamonds) are indicated for comparison ($T_L=1.7$ K). The energy-loss rates due to acoustic-phonon scattering for the parameters of samples $M1$ (solid line), $M2$ (dotted line), and $M19$ (dash-dotted line), and for the Si MOS structure (large dash-dotted line) according to our calculations and for parameters similar to samples $M1$ and $M2$ according to calculations by Shinba *et al.* (Ref. 31) (dashed line) are also shown.

V. ENERGY-LOSS RATE: ACOUSTIC PHONONS

The energy-loss rate due to acoustic-phonon scattering in two-dimensional systems, e.g., in Si MOS structures and in $GaAs/Ga_{1-x}Al_xAs$ heterostructures, has been treated by several authors.[17,19,21,31] Apart from Manion *et al.*,[19] who used a self consistently calculated wave function, all authors have so far assumed the variational ansatz of Fang, Howard, and Stern for their wave function in the lowest subband, as discussed in Ref. 32.

For the case of (001) $Si/Si_{0.7}Ge_{0.3}$ heterostructures the use of the variational wave function with a node at the interface is well justified due to the fact that the longitudinal mass $m_l=m_z=0.92m_0$ is so large that the small penetration of the wave function of the lowest electric subband into the $Si_{0.7}Ge_{0.3}$ barrier will not modify that energy-loss rate substantially. The relevant Si mass is larger by about a factor of about 14 than that of the electrons in a GaAs quantum well.

The net average energy-loss rate per electron is calculated from the energy gained by the phonons from the hot electrons. Using this approach, we write

$$\left\langle\frac{dE}{dt}\right\rangle=\int_0^\infty dE\frac{dE}{dt}f(E,T_e)\Big/\int_0^\infty dE\,f(E,T_e)\,, \quad (3)$$

where $f(E,T_e)=\{\exp[(E-E_F)/k_BT_e]+1\}^{-1}$ is the Fermi-Dirac distribution for an electron temperature T_e different from the lattice temperature. The net energy-loss rate of an electron with energy E is expressed as

$$\frac{dE}{dt}=\int_0^{2\pi}[E_+(\theta)-E_-(\theta)]d\theta\,, \quad (4)$$

with the differential energy change due to scattering of the 2D electrons with wave vector **k** expressed as

$$E_+(\theta)=\int_{-\infty}^{\infty}dq_z\hbar\omega_q|I(q_z)|^2P(q_{xy},q_z)\times N_q[1-f(E+\hbar\omega_q)] \quad (5)$$

for phonon absorption, and

$$E_-(\theta)=\int_{-\infty}^{\infty}dq_z\hbar\omega_q|I(q_z)|^2P(q_{xy},q_z)(N_q+1)\times[1-f(E-\hbar\omega_q)]\Theta(E-\hbar\omega_q) \quad (6)$$

for phonon emission. Since the differential scattering cross sections depend on the phonon energy, the phonon energy $\hbar\omega_q$ was not taken outside of the integral in the expressions for $E_+(\theta)$ and $E_-(\theta)$ [Eqs. (5) and (6)], in contrast to Ref. 17.

In Eqs. (3)–(6), θ is the scattering angle, and $E=\hbar^2k^2/2m^*$ is the electron kinetic energy, with m^* the electron in-plane effective mass m_t and $k=|\mathbf{k}|$. The phonon components parallel and normal to the heteroplane are denoted by q_{xy} and q_z, respectively. $|I(q_z)|^2$ is the form factor which describes the coupling of the electron wave function to the z component of the scattered phonon, $P(q_{xy},q_z)$ is the scattering probability factor, $N_q=[\exp(\hbar\omega_q/k_BT_L)-1]^{-1}$ the phonon occupation number, and $\Theta(E)$ the unit-step function. The phonon energy $\hbar\omega_q$ is given by $\hbar u_L q$ for longitudinal-acoustic modes. Here u_L is the longitudinal sound velocity, and $q=(q_{xy}^2+q_z^2)^{1/2}$.

The scattering probability factor for the acoustic-phonon scattering via deformation-potential coupling $P(q_{xy},q_z)$ (Ref. 17) was calculated using $c_L=1.68\times10^{11}$ N/m^2 for the longitudinal elastic constant,[33] and taking the static screening factor which was given by Hirakawa and Sakaki[34] according to the treatment originally derived by Price[35] for the screening of the deformation-potential interaction in the random-phase approximation. The deformation-potential constant for the interaction with longitudinal-acoustic (LA) modes was taken to be $D=9$ eV which is the same value as used by Stern and Laux[12] for calculating the Ohmic mobility in $Si/Si_{1-x}Ge_x$ heterostructures. For the longitudinal sound velocity an average value $u_L=8.8\times10^3$ m/s was used.

The variational parameter b (which is inversely correlated with the extension of the wave function)[32] was calculated using $\varepsilon=11.7$ for the dielectric constant, and determined to be 9.3×10^8, 8.8×10^8, and 7.3×10^8 m^{-1} for the three samples $M1$, $M2$, and $M19$, respectively.

For the LA-phonon scattering in the heterostructure, we assume that the phonon energies are those of the bulk material which forms the wells, i.e., in the $Si/Si_{1-x}Ge_x$ case we use the bulk Si phonon modes. This assumption is in agreement with calculations previously published for the energy-loss rate in Si MOS structures and $GaAs/Ga_{1-x}Al_xAs$ heterostructures. We want to point out that in the Si-based heterostructures the acoustic mismatch of the LA-phonon modes across the $Si/Si_{1-x}Ge_x$ interface is much less than for the Si MOS structures containing an amorphous oxide.

In Fig. 4 our calculated energy-loss rates for carrier concentrations and lattice temperatures corresponding to the three samples are shown. Furthermore we performed the same calculation for the energy-loss rate with parameters corresponding to a Si MOS device used by Neugebauer and Landwehr.[20] In addition, calculated data by Shinba et al.[31] for the energy-loss rate in a Si MOS device are included. The data taken from Ref. 31 are based on a calculation comparable to ours for a carrier concentration of 1.1×10^{12} cm^{-2} and $T_L=2$ K, also taking static screening effects into account. These parameters are close to those for samples $M1$ and $M2$. The results of Shinba et al.[31] for $P_E(T_e)$ agree quite well with the present ones.

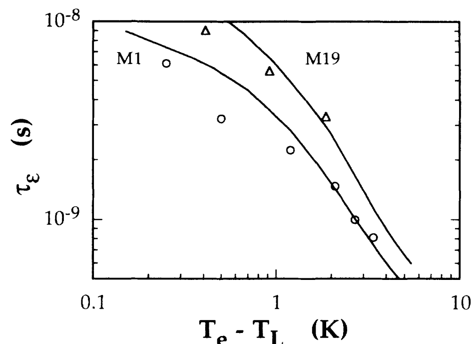

FIG. 5. Energy relaxation time τ_ε for $Si/Si_{1-x}Ge_x$ heterostructures $M1$ (open circles) and $M19$ (triangles) vs T_e-T_L as deduced from the experimentally determined energy-loss rate. Full lines: τ_ε determined from the calculated energy-loss rate.

Comparison of the calculations for samples $M1$ and $M19$, which differ by a factor of 2 in carrier concentration, shows that for a given electron temperature the loss rate increases with decreasing carrier concentration, which is due partly to the weaker screening effects. On the other hand, varying the lattice temperature and keeping the carrier concentration constant affects the loss rate substantially only at electron temperatures in the vicinity of T_L. This behavior is demonstrated by the results of the calculations for samples $M1$ and $M2$ which have quite similar carrier concentration, but for which the damping of the SdH oscillations was evaluated at lattice temperatures of 1.8 and 2.1 K. The calculated loss rates for these different lattice temperatures almost coincide for $T_e>3$ K.

It is not intended to produce a fit of the energy-loss rate vs T_e with power laws. These laws depend on approximations which are never fulfilled over an extended temperature range. However, the standard definition of an energy relaxation time "τ_ε" (see, e.g., Ref. 18) is used in order to obtain an estimate of its order of magnitude, despite the fact that it actually cannot be defined over the entire range of electron temperatures investigated here for the $Si/Si_{1-x}Ge_x$ heterostructures. The energy relaxation time is determined from

$$\tau_\varepsilon=\frac{\pi^2k_B^2}{6E_F}(T_e^2-T_L^2)P_E^{-1}\ . \qquad (7)$$

Figure 5 shows τ_ε as a function of T_e-T_L for samples $M1$ and $M19$ (which differ in carrier concentration and thus in Fermi energy by a factor of 2) together with the calculations based on Eqs. (3)–(6) for the energy-los rate. Figure 5 shows that τ_ε is about 4–2.5 orders of magnitude larger than the transport time τ_t (Table I) in the electron temperature range from 1.6 to 7 K. Even for small $(T_e$-$T_L)$ the energy relaxation time cannot be approximated by a constant value.

VI. DISCUSSION

The energy-loss rate in $Si/Si_{1-x}Ge_x$ heterostructures was determined experimentally and compared with calculated energy-loss rates due to acoustic-phonon scattering including static screening in Fig. 4. The data were taken on 2D electron gases with electron mobilities from 1.3×10^4 to 1.3×10^5 $cm^2/V\,s$. As expected from a simple electron temperature model consideration, the energy-loss rate turns out to be essentially independent of the elastic scattering mechanisms, since the experimentally determined loss rates for both high- and low-mobility samples show the same functional dependence. The experimental data for samples $M1$ and $M19$ coincide almost exactly with the calculated energy-loss data. We want to point out that this agreement is achieved without any fitting parameter. For sample $M2$ ($T_L=2.1$ K) the calculation does not differ from that for sample $M1$ ($T_L=1.8$ K) for electron temperatures above 3 K (Fig. 4). However, the experimental data differ slightly from the calculated ones. Previous calculations of the energy-loss rate by Shinba *et al.*[31] for Si MOS devices are in good agreement with the present calculated data shown in Fig. 4. Similar to the calculation presented in Sec. V for the energy-loss rate in $Si/Si_{1-x}Ge_x$ heterostructures, Shinba *et al.*[31] assumed that in Si MOS structures the two-dimensional hot carriers lose their excess energy through interaction with bulklike acoustic phonons in silicon.

Furthermore, Fig. 4 shows that the experimentally determined energy-loss rate in a Si MOS device ($\mu=4000$ $cm^2/V\,s$) (Ref. 36) at a given electron temperature according to Neugebauer and Landwehr[20] is about an order of magnitude *below* that determined for the $Si/Si_{1-x}Ge_x$ heterostructures. This result is quite astonishing. Although our calculated energy-loss rate for this Si MOS device is somewhat reduced by screening due to its higher carrier concentration of 3.7×10^{12} cm^{-2} in comparison to that of the present $Si/Si_{1-x}Ge_x$ samples (1×10^{12} and 4.7×10^{11} cm^{-2}), the calculated $P_e(T_e)$ values for this Si MOS device are considerably higher than the experimental data (see Fig. 4). In addition, we evaluated the $P_E(T_e)$ dependence from data given by Hönlein and Landwehr[36] for a Si MOS device with a carrier concentration of 2.5×10^{12} cm^{-2} and a mobility of 7000 $cm^2/V\,s$ at $T_L=2.0$ K. The energy-loss rate derived from their experimental data[36] shows almost exactly the same functional dependence as the one taken from Ref. 20 (displayed in Fig. 4). Thus for Si MOSFET's there is an apparent discrepancy between the calculated energy-loss rate (our calculation as well as that of Shinba *et al.*[31]) and the experimentally derived values.[20,36] In contrast, as shown above, there is a perfect agreement of theory and experiment for $Si/Si_{1-x}Ge_x$ heterostructures. In the following possible origins for this difference between Si MOS devices and $Si/Si_{1-x}Ge_x$ heterostructures are discussed.

To account for the lower energy-loss rate in the Si MOS device[20] in comparison to both the low- and high-mobility $Si/Si_{1-x}Ge_x$ heterostructure, one would have to decrease the value of the deformation-potential constant in the calculation substantially, i.e., to $D=3.5$ eV which is unrealistically *small.* Another possibility to explain $P_E(T_e)$ would be to assume that acoustic-phonon modes at the interface to the Si oxide differ substantially from those in bulk Si, or that long-wavelength phonons are altered by the proximity of the surface. We note that the longitudinal acoustic-phonon modes in $Si_{1-x}Ge_x$ are quite similar to those in Si, whereas this is not the case for the acoustic modes in amorphous SiO_2.

There is a further puzzle with the quantitative explanation of hot-electron transport in Si MOS devices at liquid-helium temperatures. Manion *et al.*[19] have argued that experimental data for the hot-electron mobility in Si MOS devices give evidence that the current theories of scattering in quasi-2D systems do not account properly for the deformation-potential interaction at interfaces since anomalously *large* deformation-potential constants were necessary to fit the mobility data.[37] This is in stark contrast to the energy-loss data, which require too small a deformation-potential constant. Up to now, this discrepancy has not been solved.

In the $Si/Si_{1-x}Ge_x$ samples, we did not observe any significant dependence of T_e on magnetic field B evaluated in the magnetic-field range below 2.5 or 1.5 T either for the low- or high-mobility samples. For $GaAs/Ga_{1-x}Al_xAs$ heterojunctions, Leadley *et al.*[16] reported a dependence $T_e(B)$ which was interpreted as evidence of cyclotron phonon emission. These authors reported that the cyclotron phonon emission is important for $k_B T_e > \hbar\omega_c/\lambda$, where λ is a factor between 2 and 3. If a similar condition were valid for $Si/Si_{1-x}Ge_x$ heterostructures, the effect should be observed for SdH oscillations below 0.6 T in our samples. However, for the $Si/Si_{1-x}Ge_x$ samples investigated the Dingle temperature is too large even in the high-mobility sample $M19$, and thus the magnetoresistance does not show oscillations below $B=0.6$ T at $T_L=1.55$ K. For higher electron temperatures the condition $k_B T_e > \hbar\omega_c/\lambda$ cannot be fulfilled since the SdH oscillations vanish in the corresponding low-magnetic-field range. In Si MOS structures cyclotron phonon emission was observed by Challis and Kent[38] by a thermal detection of the emitted phonon intensity as a function of gate voltage.

Apart from the excellent agreement between calculated and experimentally observed dependences $P_E(T_e)$ for the $Si/Si_{1-x}Ge_x$ heterostructures, we have recently obtained further support for the use of the electron temperature model at these low lattice temperatures and comparatively small applied electric fields. From experiments on the weak localization effect on sample $M2$, the temperature dependence of the phase coherence time was deduced, and found to be in the range of about 1 ps for temperatures between 1.8 and 4.2 K.[39] This phase coherence time is determined by inelastic electron-electron-scattering processes. Its value is comparable to the transport (momentum relaxation) time, and both are about two to three orders of magnitude smaller than the energy relaxation time. Therefore the use of a Fermi distribution function with an electron temperature higher than

the lattice temperature is appropriate.

Besides the high-field transport properties, there are apparent differences in the Ohmic transport in Si MOS devices and $Si/Si_{1-x}Ge_x$ heterostructures. As pointed out by Gold,[13] the limiting scattering mechanism for the Ohmic mobility of the 2DEG in the Si channel is due to interface charges. The highest electron mobility (4×10^4 $cm^2/V\,s$) reported so far for Si MOS devices corresponds to about 10^{10} interface charged per cm^2. Naturally, interface charges are less important in $Si/Si_{1-x}Ge_x$ heterostructures. As already pointed out, remote impurity scattering is the dominant scattering mechanism in high-mobility $Si/Si_{1-x}Ge_x$ samples ($\mu > 10^5$ $cm^2/V\,s$, $\tau_t/\tau_s \approx 10$) according to Stern and Laux.[12]

The factor of 10 variation in the Ohmic mobilities in the present $Si/Si_{0.7}Ge_{0.3}$ samples results both from different buffer layer thicknesses and the reduction of remote impurity scattering due to different spacer layer thicknesses. Nelson *et al.*[40] have shown that the change of the buffer layer thickness is accompanied by a drastic increase of the correlation length of surface roughness from about 50 to 1000 Å, when comparing samples $M1$ and $M2$ on the one hand, and $M19$ on the other. Similar phenomena were reported by Xie *et al.*[4] Our experimental energy-loss rate data on the three $Si/Si_{1-x}Ge_x$ samples now prove that the interface roughness does not influence the functional dependence of $P_E(T_e)$ in the range of electric fields investigated.

VII. CONCLUSION

The energy-loss rate for hot electrons in $Si/Si_{1-x}Ge_x$ modulation-doped heterostructures was obtained as a function of the electron temperature in the range from 1.6 to 7 K. The damping of Shubnikov–de Haas oscillation amplitudes with applied electric field was used to experimentally determine the electron temperature. These experiments were compared with calculations of the energy-loss rate for carrier scattering by acoustic phonons via the deformation-potential coupling, taking static screening of the electron-phonon interaction into account. The calculations of the energy-loss rates reproduce the observed dependence $P_E(T_e)$ in all three samples without any fit parameter, despite the fact that their mobilities vary from 1.3×10^4 to 1.3×10^5 $cm^2/V\,s$. These results demonstrate that the energy-loss rate does not depend on the elastic-scattering processes (remote ionized impurity scattering and interface roughness scattering) which limit the electron mobility in the range of electron temperatures investigated.

ACKNOWLEDGMENTS

This work was supported by Project No. GZ 601.528/2-26/92 of "Bundesministerium für Wissenschaft und Forschung", Vienna. We thank M. Helm for a critical reading of the manuscript.

---

*Present address: Dept. of Electronics, Faculty of Engineering, Cairo University, Egypt.

[1]For a recent review see, e.g., H. Presting, H. Kibbel, M. Jaros, R. M. Turton, U. Menczigar, G. Abstreiter, and H. G. Grimmeis, Semicond. Sci. Technol. **7**, 1127 (1992).

[2]K. Ismail, B. S. Meyerson, and P. J. Wang, Appl. Phys. Lett. **58**, 2117 (1991).

[3]S. F. Nelson, K. Ismail, J. O. Chu, and B. S. Meyerson, Appl. Phys. Lett. **63**, 367 (1993).

[4]Y. H. Xie, E. A. Fitzgerald, D. Monroe, P. J. Silverman, and G. P. Watson, J. Appl. Phys. **73**, 8364 (1993).

[5]G. L. Patton, J. H. Comfort, B. S. Meyerson, E. F. Crabbe, G. J. Scilla, E. DeFresart, J. M. C. Stork, J. Y. C. Sun, D. L. Harame, and J. Burghartz, Electron. Device Lett. **11**, 171 (1990).

[6]K. Ismail, B. S. Meyerson, S. Rishton, J. Chu, S. Nelson, and J. Nocera, IEEE Electron. Device Lett. **13**, 229 (1992).

[7]E. Crabbé, B. Meyerson, D. Harame, J. Stork, A. Megdanis, J. Cotte, J. Chu, M. Gilbert, C. Stanis, J. Comfort, G. Patton, and S. Subbanna (unpublished).

[8]F. Schäffler and U. König, in *Low-Dimensional Electronic Systems,* edited by G. Bauer, F. Kuchar, and H. Heinrich, Springer Series in Solid State Sciences Vol. 111 (Springer, New York, 1992), p. 354.

[9]H. Daemkes, H. J. Herzog, H. Jorke, H. Kibbel, and E. Kaspar, IEEE Trans. Electron, Devices **ED-33**, 633 (1986).

[10]G. Abstreiter, H. Brugger, T. Wolf, H. Jorke, and H. J. Herzog, Phys. Rev. Lett. **54**, 2441 (1985).

[11]G. Abstreiter, in *Low-Dimensional Electronic Systems* (Ref. 8), p. 323.

[12]F. Stern and S. E. Laux, Appl. Phys. Lett. **61**, 1110 (1992).

[13]A. Gold, Phys. Rev. B **35**, 723 (1987); Phys. Rev. Lett. **54**, 1079 (1985).

[14]G. Bauer and H. Kahlert, Phys. Rev. B **5**, 566 (1972).

[15]B. K. Ridley, Rep. Prog. Phys. **54**, 169 (1991).

[16]D. R. Leadley, R. J. Nicholas, J. J. Harris, and C. T. Foxon, Semicond. Sci. Technol. **4**, 879 (1989).

[17]K. Hirakawa and H. Sakaki, Appl. Phys. Lett. **49**, 889 (1986).

[18]J. Lutz, F. Kuchar, K. Ismail, H. Nickel, and W. Schlapp, Semicond. Sci. Technol. **8**, 399 (1993).

[19]S. J. Manion, M. Artaki, M. A. Emanuel, J. J. Coleman, and K. Hess, Phys. Rev. B **35**, 9203 (1987).

[20]T. Neugebauer and G. Landwehr, Phys. Rev. B **21**, 702 (1980).

[21]K. Hess, T. Englert, T. Neugebauer, G. Landwehr, and G. Dorda, Phys. Rev. B **16**, 3652 (1977).

[22]R. Fletcher, J. J. Harris, C. T. Foxon, and R. Stoner, Phys. Rev. B **45**, 6659 (1992).

[23]S. F. Nelson, K. Ismail, J. J. Nocera, F. F. Fang, E. E. Mendez, J. O. Chu, and B. S. Meyerson, Appl. Phys. Lett. **61**, 64 (1992).

[24]L. M. Roth and P. N. Argyres, in *Semiconductors and Semimetals,* edited by R. K. Willardson and A. C. Beer (Academic, New York, 1966), Vol. 1 , p. 159.

[25]C. I. Harris, B. Monemar, G. Brunthaler, H. Kalt, and K. Köhler, Phys. Rev. B **45**, 4227 (1992).

[26]S. Das Sarma and F. Stern, Phys. Rev. B **32**, 8442 (1985).

[27]P. T. Coleridge, R. Stoner, and R. Fletcher, Phys. Rev. B **39**, 1120 (1989).

[28]D. Többen, F. Schäffler, A. Zrenner, and G. Abstreiter, Phys. Rev. B **46**, 4344 (1992).

[29]A. V. Akimov, L. J. Challis, J. Cooper, C. J. Mellor, and E. S. Moskalenko, Phys. Rev. B **45**, 11 387 (1992).

[30]K. Hess (private communication).
[31]Y. Shinba, K. Nakamura, M. Fukuchi, and M. Sakata, J. Phys. Soc. Jpn. **51**, 157 (1982).
[32]F. Stern, Phys. Rev. B **5**, 4891 (1972).
[33]W. Kress, in *Numerical Data and Functional Relationships in Science and Technology,* edited by O. Madelung, Landolt-Börnstein, New Series, Group IV, Vol. 17, Pt. a (Springer-Verlag, Berlin, 1982), pp. 46–63.
[34]K. Hirakawa and H. Sakaki, Phys. Rev. B **33**, 8291 (1986).
[35]P. J. Price, Ann. Phys. (N.Y.) **133**, 217 (1981); J. Vac. Sci. Technol. **19**, 599 (1981); J. Appl. Phys. **53**, 6863 (1982).
[36]W. Hönlein, and G. Landwehr, J. Phys. (Paris) C 7, 25 (1981).
[37]Y. Shinba and K. Nakamura, J. Phys. Soc. Jpn. **50**, 114 (1981).
[38]L. J. Challis and A. J. Kent (Ref. 8), p. 31.
[39]G. Stöger, G. Brunthaler, G. Bauer, K. Ismail, B. S. Meyerson, J. Lutz, and F. Kuchar, Semicond. Sci. Technol. (to be published).
[40]S. F. Nelson, K. Ismail, T. N. Jackson, J. J. Nocera, J. O. Chu, and B. S. Meyerson, Appl. Phys. Lett. **63**, 794 (1993).